



DE GRUYTER
OPEN

FLUID
MECHANICS

DOI: 10.2478/jtam-2014-0024

NONLINEAR STABILITY OF FREE THIN FILMS:
THERMOCAPILLARY AND VAN-DER-WAALS EFFECTS*

S. TABAKOVA

*Department of Mechanics, TU – Sofia, branch Plovdiv,
25, Tzanko Djustabanov, BG-4000 Plovdiv, Bulgaria,
Department of Fluid Mechanics, Institute of Mechanics, BAS,
Acad. G. Bontchev St., Bl. 4, 1113 Sofia, Bulgaria
e-mail: stabakova@gmail.com*

S. RADEV

*Department of Fluid Mechanics, Institute of Mechanics, BAS,
Acad. G. Bontchev St., Bl. 4, 1113 Sofia, Bulgaria
e-mail: stradev@imbm.bas.bg*

[Received 04 November 2014. Accepted 17 November 2014]

ABSTRACT. In the present work the dynamics of a non-isothermal thin viscous film, with fully mobile interfaces, is studied in the case when the inertial, viscous, capillary, van der Waals and thermocapillary forces are important. The film is laterally bounded by a frame, whose temperature is higher than the environmental one. The stability of the static film shapes is examined numerically by a linear and non-linear analysis. The results show that the film rupture is mostly governed by the dynamics, but it could be delayed or enhanced by the thermocapillary convection and the heat transfer with the surrounding environment.

KEY WORDS: free thin film, heat transfer, thermocapillary convection, van-der-Waals force, linear stability, non-linear stability.

1. Introduction

The isothermal behaviour of thin films (free or supported) has been extensively investigated for many years by different authors [1], [2]. However,

*Corresponding author e-mail: stabakova@gmail.com.

This paper is an enlarged variant to a paper presented at the 12th National Congress of Theoretical and Applied Mechanics, 23–26 September, 2013, Saints Constantine and Elena, Varna, Bulgaria.

One of the authors (S. R.) kindly acknowledges the financial support of Bulgarian Research Fund in the frames of the Project DCVP 02/1.

the non-isothermal case has received less attention although the variety of its applications in the modern technologies: ink-jet printing (the thin films could be regarded as a Cartesian approach of the thin jets); large glass sheets for the LCD displays; solidifying slices of semiconductor materials for the electronic microchips; etc.

The influence of the free film dynamics on the heat transfer and solidification at a radiation transfer from the film interfaces has been studied numerically in [3], [4]. However in these works the stability questions have not been treated. In a recent paper [5] the long-wave analysis has been applied for an infinite free viscous sheet with a given temperature different from the ambient one. The authors show that there exists a stable thermal mode coupled to the dynamical modes obtained by the linear stability analysis. This coupling can promote or delay the onset of the film rupture, if a convenient phase shift to the initial temperature profile with respect to the initial velocity profile is applied.

In the present work, the non-isothermal free film dynamics is studied. A linear stability analysis is implemented numerically by the method of the differential Gauss elimination like in our previous works [6], [7]. It is found that the film will be less stable with the increase of the thermocapillary convection and heat transfer with the surrounding gas. Similar results are obtained by the non-linear stability analysis, from which the evolution of the film thickness, lateral velocity and temperature is also found.

2. Problem statement

The film fluid is supposed Newtonian viscous with constant physical properties: density ρ , dynamic viscosity μ , thermal conductivity κ , heat capacity c and heat transfer coefficient with the ambient gas β . The surface tension σ depends on the film temperature θ as: $\sigma = \sigma_0 - \gamma(\theta - \theta_0)$, where γ is the rate of the surface tension dependence on the temperature. The film drains because of the inertia, viscosity, thermocapillary convection and van-der-Waals force acting as a disjoining pressure. The heat transfer is supposed to be due to the conduction, convection inside the film and heat transfer with the surrounding gas, whose temperature is θ_0 . The film is assumed symmetrical with respect to its central plane $z = 0$ and laterally bounded by a solid rectangular frame, hotter than the ambient. Thus the frame temperature θ_1 is different from θ_0 , i.e., $\theta_1 > \theta_0$. The film can be considered as one dimensional (in x direction), if one side of the frame is much longer than the other. The average film thickness \bar{h} is assumed to be much smaller than the shorter frame side a , such that $\bar{h} = \varepsilon a$,

where $\varepsilon \ll 1$. The free symmetrical surfaces are defined as $z = \pm h'/2$, where $h'(x, t) = O(\varepsilon)$ represents the film shape. Next, the following characteristic scales will be used: a for the lateral length, U for the lateral velocity, a/U for the time, $\Delta\theta = (\theta_1 - \theta_0)$ for the temperature and εa for the film thickness.

The coupled thermal-dynamic system in dimensionless form for the film thickness $h = h'/\varepsilon a$, longitudinal velocity u and temperature $T = \frac{\theta - \theta_0}{\theta_1 - \theta_0}$ is given by (similarly as in [3], [4], [5]):

$$(2.1) \quad \frac{\partial h}{\partial \tau} + \frac{\partial}{\partial x}(uh) = 0,$$

$$(2.2) \quad \frac{\partial u}{\partial \tau} + u \frac{\partial u}{\partial x} = \frac{\varepsilon}{We} \frac{\partial^3 h}{\partial x^3} + \frac{4}{Re} \frac{\partial}{\partial x} \left(h \frac{\partial u}{\partial x} \right) + \frac{A}{h^4} \frac{\partial h}{\partial x} - \frac{2M}{h} \frac{\partial T}{\partial x},$$

$$(2.3) \quad \frac{\partial T}{\partial \tau} + u \frac{\partial T}{\partial x} = \frac{1}{Pe h} \frac{\partial}{\partial x} \left(h \frac{\partial T}{\partial x} \right) - \frac{Bi}{Pe h} T,$$

where τ is the dimensionless time, $Re = \rho a U / \mu$ is the Reynolds number, $We = 2\rho a U^2 / \sigma_0$ is the Weber number, $A = \frac{A_H}{2\pi \rho U^2 a^3 \varepsilon^3}$ is the dimensionless Hamaker constant (A_H being the dimensional Hamaker constant), $M = \frac{1}{\varepsilon We} \frac{\gamma}{\sigma_0} \Delta\theta$ is the Marangoni number, $Pe = Pr Re$ is the Peclet number, $Pr = c\mu/\kappa$ is the Prandtl number and $Bi = \frac{2\beta a}{\varepsilon \kappa}$ is the Biot number.

The boundary conditions for h , u and T on the frame are the wetting condition for the film shape h , the no-slip condition for the lateral velocity u and the constant temperature condition, i.e.:

$$(2.4) \quad \frac{\partial h}{\partial x}(\pm 1, \tau) = \pm \tan \alpha, \quad u(\pm 1, \tau) = 0, \quad T(\pm 1, \tau) = 1,$$

where $\pi/2 - \arctan(0.5 \tan \alpha)$ is the wetting angle with the frame (Note, that for the planar films $\alpha = 0$, as the wetting angles are right angles.).

The mass (volume) conservation condition reads:

$$(2.5) \quad \int_{-1}^1 h dx = W,$$

where $W = const$ is the initial film volume (here taken $W = 2$, correspondent to a planar film with a dimensionless thickness $h = 1$).

Since the system (2.1)–(2.3) is of $O(\varepsilon)$, the dimensionless numbers are limited as: $Re \leq \varepsilon^{-1}$, $We \leq 1$ and $Pe \leq \varepsilon^{-1}$. Usually the water films of mean thickness of $O(10^{-5}m)$ attached on frames with sides of $O(10^{-2}m)$ enter into these restrictions.

3. Results

3.1. Film relaxation and drainage

If the complementary wetting angle is zero, $\alpha = 0$, then there exists an analytical static solution of the system (2.1)–(2.3) $h_s = 1, T_s = 1$ that refers only to the adiabatic case, i.e., at $Bi = 0$. If $M = 0$ (the constant surface tension case) and $Bi \neq 0$ the system (2.1)–(2.3) has also the static solution $h_s = 1$, but with $T = \frac{\text{ch}(\sqrt{Bi}x)}{\text{ch}(\sqrt{Bi})}$. For larger angles $\alpha > 0$, the static solution can only be obtained as a numerical solution of the dynamical problem at given initial conditions, for example: $h_0(x) = 1, u_0(x) = 0, T_0(x) = 0$. It is found that the static shapes exist only for some combinations of the problem parameters (for some values of B, α, Ma and Bi , where $B = WeA/\varepsilon$ and $Ma = WeM/\varepsilon$ [6]). For example, at $B \geq 9$, the static film shapes exist only for $\alpha = 0$, while at $B = 0.01$ – for $0 \leq \alpha \leq 1.37$. If the film shape is static for $Ma = Bi = 0$, it remains also static at different values of Ma and Bi .

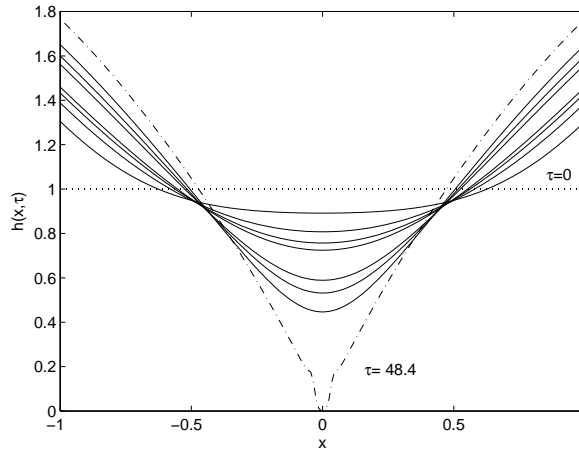


Fig. 1. Thin film evolution in successive times starting from a planar shape at $\tau = 0$ for $\alpha = 0.85, Re = Pe = 1, We = 0.01, \varepsilon = 0.01, A = 3$ ($B = 3$): a) “pimple” rupture in $x = 0$ and $\tau = 48.4$ for $Ma = 0, Bi = 0$ (0.1, 1) (The final shapes are plotted as “dash-dotted” lines, the initially disturbed states – as “dotted” lines)

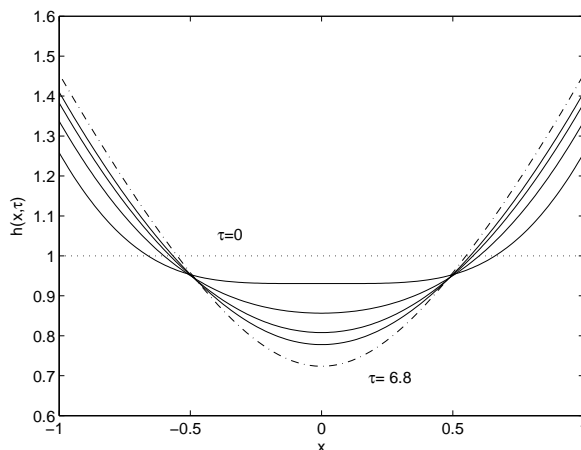


Fig. 1. b) static film shape reached at $\tau = 6.8$ for $Ma = 1$, $Bi = 1$.

Contrary, if at $Ma = Bi = 0$ the film ruptures, the increase of Ma and Bi increases the rupture time and even a static shape could be reached.

An example for the film shape evolution is shown in Fig. 1 for $\alpha = 0.85$ at $Ma = 0$, $Bi = 0$ (plot (a)) and $Ma = 1$, $Bi = 1$ (plot (b)). The rupture time is $\tau = 48.4$ for the case on plot (a) and the relaxation time (the time to reach the static shape) is $\tau = 6.8$ for the case on plot (b). We have to note that the rupture time at $Ma = 0$ and $Bi = 0$ remains the same with the change of Bi , as the heat transfer is separated from the film dynamics and the final temperature remains constant ($T = 1$). The increase of Ma leads to a competition between the Marangoni stresses and the van-der-Waals force, as the latter is responsible for the film rupture. For example, in the case shown in Fig. 1b), the temperature tends to its static profile.

3.2. Linear stability

Let some small disturbances $\tilde{h}(x, \tau)$, $\tilde{u}(x, \tau)$ and $\tilde{T}(x, \tau)$ are imposed on the static state solutions:

$$(3.1) \quad h = h_s + \tilde{h}, \quad u = \tilde{u}, \quad T = T_s + \tilde{T}.$$

Further, the disturbances \tilde{h} , \tilde{u} and \tilde{T} are sought as exponential functions in time with an unknown growth rate $\omega = \omega_r + i\omega_i$ and unknown distributions $H(x)$, $V(x)$ and $G(x)$:

$$(3.2) \quad \tilde{h} = H(x) \exp(\omega\tau), \quad \tilde{u} = V(x) \exp(\omega\tau), \quad \tilde{T} = G(x) \exp(\omega\tau).$$

After inserting (3.1) with (3.2) in Eqs (2.1)–(2.3), neglecting the 2nd order disturbances, a characteristic system for ω is obtained:

$$(3.3) \quad \omega H = -(h_s V)'$$

$$(3.4) \quad \omega V = \frac{\varepsilon}{We} H''' + \frac{4}{Re h_s} (h_s V')' - \frac{2M}{h_s} G' + \frac{A}{h_s^4} H' + \left(\frac{2MT'_s}{h_s^2} - \frac{4Ah'_s}{h_s^5} \right) H$$

$$(3.5) \quad \omega G = -T'_s V + \frac{1}{Pe h_s} (h_s G')' + \frac{1}{Pe h_s} (T'_s H)' - \frac{Bi}{Pe h_s} G - \frac{[(h_s T'_s)' - Bi T'_s]}{Pe h_s^2} H$$

with boundary conditions:

$$(3.6) \quad H'(\pm 1) = 0, \quad V(\pm 1) = 0, \quad G(\pm 1) = 0.$$

At $\alpha = 0$ and $Bi = 0$, the upper system turns into an algebraic equation of 3rd degree for ω , independent of the Marangoni number M , which is similar to the characteristic equation in the case of an infinite liquid sheet [5]:

$$(3.7) \quad \omega^3 + \left(\frac{4}{Re} + \frac{1}{Pe} \right) m^2 \omega^2 + \left[\frac{4m^2}{Re Pe} + \frac{\varepsilon}{We} (m^2 - B) \right] m^2 \omega + \frac{\varepsilon}{Pe We} (m^2 - B) m^4 = 0$$

This equation has one negative root connected to the thermal mode, $\omega_1 = -m^2/Pe$ and two other roots (a negative one and the other one is positive or negative, depending on B), $\omega_{2,3} = \frac{-2m^2}{Re} \left[1 \mp \sqrt{1 - \frac{\varepsilon Re^2 (m^2 - B)}{4 We m^2}} \right]$, where m is the wave number. The cutoff wave number $m_c = \sqrt{B}$, at which $\omega_2 = 0$, is the same as it has been found in the isothermal case by many authors [8] and also in our previous works [6], [7]. Thus, for the plane static films, the thermal instability always decays in time, while the film shape instability may rupture the film.

In the case of $\alpha > 0$ the characteristic system for ω has no analytical solution. It is solved numerically by the secant method and the differential Gauss elimination method that have been applied to the case of an isothermal film in [6], [7]. Details of this method are given in the Appendix.

The numerically found eigenvalues $\Omega_r = \omega_r We / \varepsilon Re$ (the imaginary part is zero, $\omega_i = 0$) are presented in Fig. 2 as functions of α , Ma and Bi at

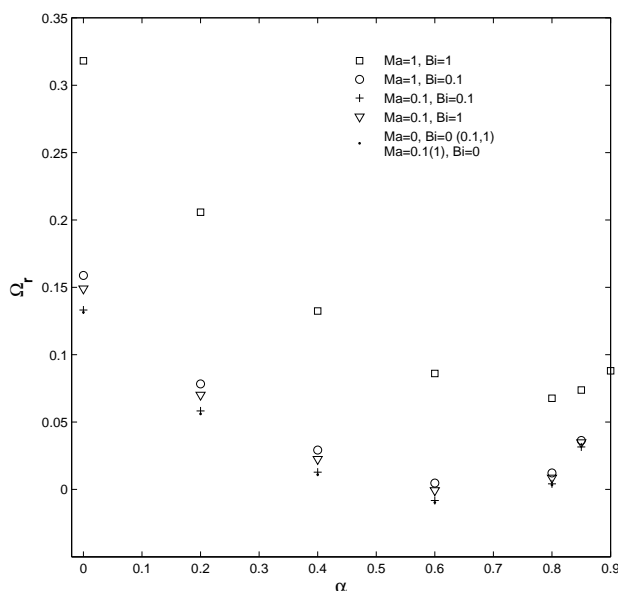


Fig. 2. Eigenvalues Ω_r at $Re = Pe = 1$, $We = \varepsilon = 0.01$ and $B = 3$ as functions of α , $Ma = 0; 0.1; 1$ and $Bi = 0; 0.1; 1$. ($\Omega_r = \omega_r We / \varepsilon Re$)

$Re = Pe = 1$, $We = \varepsilon = 0.01$ and $B = 3$. The value of $\Omega_r = 0.1314$ at $\alpha = 0$, $Ma = 0$ and $Bi = 0$ is confirmed by the root ω_2 at $m = \pi/2$ ($m = \pi/2 < m_c = \sqrt{3}$ corresponds to the unstable mode). From these results, it is clear that for all values of $Ma = 0; 0.1; 1$ and $Bi = 0; 0.1; 1$ the film is unstable, except for $\alpha = 0.6$ at $Bi = 0$ or at $Bi > 0$ and $Ma < 1$. It can be concluded that the bigger Ma , i.e., the higher temperature difference $\Delta\theta$ or the higher surface tension rate γ , will promote instability leading to rupture.

3.3. Non-linear stability

The non-linear stability analysis is based on the numerical solution of the thermo-dynamical problem (2.1)–(2.5) with different initial conditions. Here, we shall concentrate on those initial conditions correspondent to the “most dangerous” wave number $m = \pi/2$:

1. asymmetrical disturbances applied only on the film static shape h_s :

$$(3.8) \quad h_0(x) = h_s(x) + 0.1 \sin(\pi x/2), \quad u_0(x) = 0, \quad T_0(x) = T_s(x);$$

2. symmetrical disturbances applied on the static (zero) velocity:

$$(3.9) \quad h_0(x) = h_s(x), \quad u_0(x) = 0.1 \cos(\pi x/2), \quad T_0(x) = T_s(x);$$

3. symmetrical disturbances applied on the static (zero) velocity and on the static temperature T_s with (or without) phase shift $\delta\pi/2$, where $\delta = 0; \pm 1$:

$$(3.10) \quad \begin{aligned} h_0(x) &= h_s(x), u_0(x) = 0.1 \cos(\pi x/2), \\ T_0(x) &= T_s(x) + 0.1 \cos(\pi/2(x + \delta)), \end{aligned}$$

In the first case of disturbance a different film behavior is observed when changing the parameters α, Ma and Bi at given values of the rest parameters. Example results at $Re = Pe = 1, We = 0.01, \varepsilon = 0.01, A = 3 (B = 3)$ are systemized on Table 1.

Table 1. Time of rupture τ_{rup} and point of rupture x_{rup} at $Re = Pe = 1, We = 0.01, \varepsilon = 0.01, A = 3 (B = 3)$ and initial shape disturbance (case 1)

Ma, Bi	$Ma, Bi=0$	$Ma=Bi=0.1$	$Ma=1, Bi=0.1$	$Ma=0.1, Bi=1$	$Ma=Bi=1$
	τ_{rup}/x_{rup}	τ_{rup}/x_{rup}	τ_{rup}/x_{rup}	τ_{rup}/x_{rup}	τ_{rup}/x_{rup}
$\alpha = 0$	6.5/-1	6.5/-1	6/-1	6.2/-1	4/-1
$\alpha = 0.6$	static	static	118.2/-0.425	static	25.2/-0.525
$\alpha = 0.8$	52.9/-0.185	53.1/-0.195	53.9/-0.205	53.8/-0.205	37.9/-0.315

It is interesting to note that including a thermo-capillary convection and/or heat transfer with the ambient air, expressed by different values of Ma and Bi , the film with a wetting angle $90^\circ (\alpha = 0)$ with the lateral boundary (it could be also an infinite periodic film) will always rupture, if it ruptures when is isothermal. The same concerns also a greater part of the other wetting angles. However, there exist some wetting angles for which the film returns to its static shape for smaller values of Ma , but with the increase of the thermo-capillary convection, i.e., with Ma , the film ruptures. There is no influence of the heat transfer on the film behavior type. Both Ma and Bi almost always intensify the rupture process, i.e., shorten the rupture time and move the rupture point towards the left boundary point. It can be seen that the predictions of the linear stability analysis displayed in Fig. 2 are confirmed by the non-linear analysis results given on Table 1.

In Fig. 3a), b) the film thickness rupture is shown at $Re = Pe = 1, We = 0.01, \varepsilon = 0.01, A = 3 (B = 3), Ma = 1$ and $Bi = 1$ for $\alpha = 0.6$ and $\alpha = 0.8$, respectively. The rupture takes place at different points x and

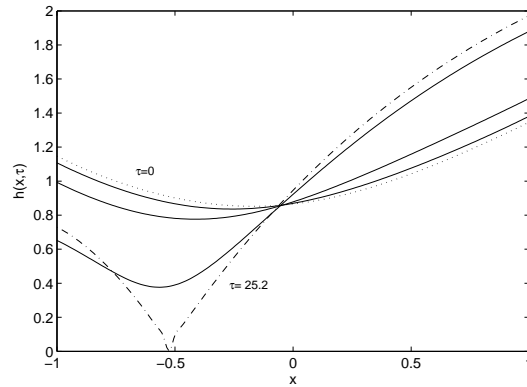


Fig. 3. Rupture of a free film at $Re = Pe = 1$, $We = 0.01$, $\varepsilon = 0.01$, $A = 3$ ($B = 3$), $M = Ma = 1$, $Bi = 1$ after applying the initial disturbance $h(x, 0) = h_s(x) + 0.1 \sin(\pi/2x)$ on its static shape $h_s(x)$: a) the film shape $h(x, \tau)$ for $\alpha = 0.6$. (The final states are plotted as “dash-dotted” lines, the initially disturbed states – as “dotted” lines.)

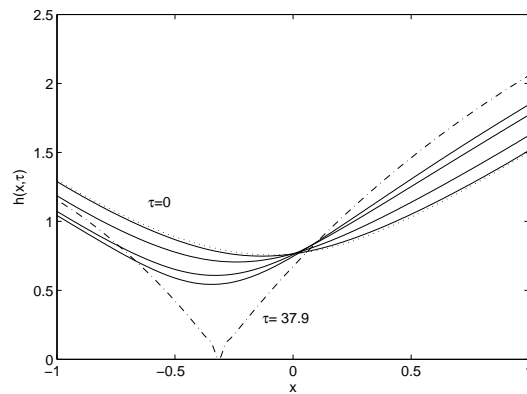
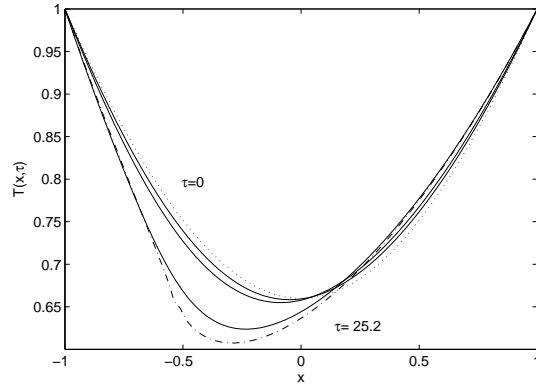
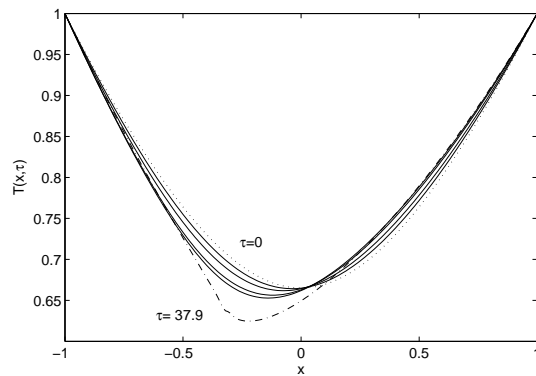


Fig. 3 b) the film shape $h(x, \tau)$ for $\alpha = 0.8$

times τ : at $x = -0.525$ and $\tau = 25.2$ for $\alpha = 0.6$ and at $x = -0.315$ and $\tau = 37.9$ for $\alpha = 0.8$. The corresponding temperature profiles for the same cases are plotted in Fig.3c), d) and show asymmetrical final temperature profiles (although starting from initially symmetrical static temperature profiles).

In the second considered case of disturbances, when only the velocity is disturbed, the rupture time is increasing with respect to the results of the first case of film shape disturbances. For example at $\alpha = 0$, $Ma = 1$, $Re = Pe = 1$,

Fig. 3 c) the temperature $T(x, \tau)$ for $\alpha = 0.6$ Fig. 3. d) the temperature $T(x, \tau)$ for $\alpha = 0.8$

$We = 0.01$, $\varepsilon = 0.01$ and $A = 3$ ($B = 3$), the rupture times become $\tau = 18.3$ for $Bi = 0.1$ and $\tau = 11.1$ for $Bi = 1$, which are longer than the rupture times at the same parameters, but at initial disturbances of the film shape only, as seen on Table 1.

In the third case of the initial disturbances a delay of the rupture or a rapid return to the static shape is found. Typical examples are given on Table 2 for some values of the parameters: $Re = Pe = 1$, $We = 0.01$, $\varepsilon = 0.01$, $A = 3$ ($B = 3$), $Ma = 1$ and $Bi = 0.1$ or 1 , for $\alpha = 0, 0.2$ and 0.8 . It is evident that for all wetting angles the time for film rupture is shorter if there is a positive phase shift of the temperature disturbance with respect to the velocity one. However, for the negative phase shift the rupture time is longer or even the

rupture could be avoided, i.e., the film reaches its static shape (at $\alpha = 0.8$ and $Bi = 1$). The respective rupture points remain unchanged for the different phase shifts. In Fig.4a), b) the film shape and temperature are displayed for the same values of the parameters as of Table 2 and at $\alpha = 0.8$, $Bi = 1$ and $\delta = 1$. It is well seen that the film final shape and the final temperature profile (at the rupture time) are the same as in Fig.3b), d), although that obtained at different initial disturbances. The eventual delay or enhancement of the rupture onset by the initial thermal disturbances, which are in a phase shift with respect to the velocity disturbances, is a new result that has been recently observed also in [5] for an infinite periodic film.

Table 2. Time of rupture τ_{rup} and point of rupture x_{rup} at $Re = Pe = 1$, $We = 0.01$, $\varepsilon = 0.01$, $A = 3$ ($B = 3$), $Ma = 1$ and initial velocity and temperature disturbances (case 3)

α	Bi	$\delta = -1$	$\delta = 1$	$\delta = 0$
		τ_{rup}/x_{rup}	τ_{rup}/x_{rup}	τ_{rup}/x_{rup}
0	0.1	20.1/-1	16.8/-1	18.4/-1
0	1	12.1/-1	10.4/-1	11.2/-1
0.2	0.1	43.7/-0.845	35.9/-0.845	39.5/-0.845
0.2	1	22.3/-0.915	19.0/-0.915	20.6/-0.915
0.8	1	static	182.7/-0.315	204.4/-0.315

4. Conclusions

In the present paper we study both the dynamics of a non-isothermal free thin viscous film, attached on a rectangular frame, and the role of the heat transfer on its stability. The van-der-Waals attractive disjoining pressure and the Marangoni thermo-capillary convection are taken into account. An evolutionary system consisting of three coupled non-linear PDE for the film thickness, lateral velocity and temperature describes the considered thermodynamical process. In the general case of the problem parameters, its solution has been obtained numerically. Since the film relaxation leads to two different final states: static film shape and film rupture, the increase of the Marangoni number could change the rupture state into a static one when the other parameters are left the same. For the obtained static shapes, a linear stability analysis is implemented numerically by the method of the differential Gauss elimination. It is found that the instability growth rate is positive and increases with the increase of the Marangoni number for almost all the wetting angles at the

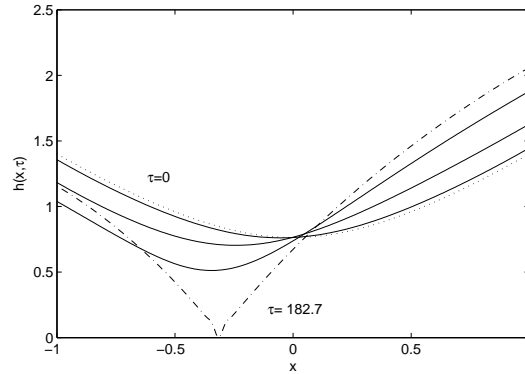


Fig. 4. Rupture of a free film at $Re = Pe = 1$, $We = 0.01$, $\varepsilon = 0.01$, $A = 3$ ($B = 3$), $M = Ma = 1$, $Bi = 1$ and $\alpha = 0.8$ after applying the initial disturbance $u_0(x) = 0.1 \cos(\pi/2x)$, $T_0(x) = T_s(x) + 0.1 \cos(\pi/2(x+1))$ on its static state: a) the film shape $h(x, \tau)$. (The final states are plotted as “dash-dotted” lines, the initially disturbed states – as “dotted” lines.)

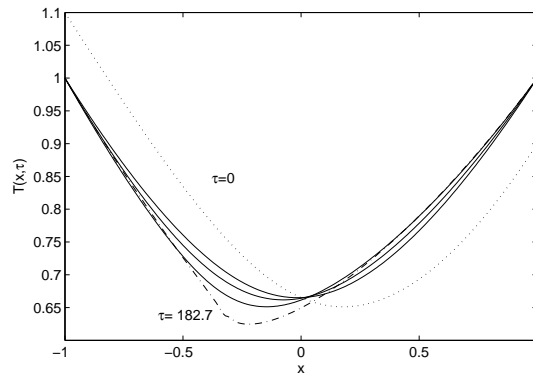


Fig. 4. b) the temperature profile $T(x, \tau)$

considered values of the parameters. These results are approximately confirmed by the results of the non-linear stability analysis, from which the evolution of the film thickness, lateral velocity and temperature distribution are found. The importance of the wetting angle is confirmed: the film can be stable or unstable depending on the competition between the wetting with the lateral boundary (frame), the thermo-capillary convection and the van-der-Waals attraction. An idea to control the rupture process by appropriate initial thermal disturbances is proposed, which will be further developed in our future studies.

Appendix A

Instead of the disturbance functions $H(x)$, $V(x)$ and $G(x)$, new variables are introduced by:

$$(A.1) \quad \mathbf{v} = (v_1, v_2, v_3) = (h_s V', (h_s V)''' - \Omega V', \Omega G'),$$

$$(A.2) \quad \mathbf{w} = (w_1, w_2, w_3) = (h_s V, (h_s V)'' - \Omega V, \Omega G),$$

where $\Omega = C\omega$ and $C = \frac{We}{\varepsilon Re}$.

Then the system of Ordinary Differential Equations (ODE) (3.3)–(3.5) is transformed into a linear ODE system of 1st order:

$$(A.3) \quad \mathbf{v}' = \mathbf{K}\mathbf{v} + \mathbf{G}\mathbf{w},$$

$$(A.4) \quad \mathbf{w}' = \mathbf{D}\mathbf{v} + \mathbf{E}\mathbf{w},$$

where

$$\mathbf{G} = \begin{pmatrix} -\frac{\Omega}{h_s^2}(3h_s'' - 3\Omega + \frac{\Omega h_s}{C} + \frac{B}{h_s^3}) + \frac{4Bh_s'^2}{h_s^6} - \frac{2Mah_s'T_s'}{h_s^3} & 1 & 0 \\ \left(Pe + \frac{C}{h_s}\right)\frac{T_s'\Omega}{h_s} - \frac{Ch_s'^2 T_s'}{h_s^3} + \frac{BiCh_s'T_s}{h_s^3} & \frac{3\Omega}{h_s} - \frac{B}{h_s^4} & 0 \\ & \frac{CT_s'}{h_s} & \frac{Pe\Omega}{C} + \frac{Bi}{h_s} \end{pmatrix},$$

$$\mathbf{K} = \begin{pmatrix} -\frac{h_s'}{h_s} & 0 & 0 \\ -\frac{2\Omega h_s'}{h_s^2} + \frac{4Bh_s'}{h_s^5} - \frac{2MaT_s'}{h_s^2} & 0 & \frac{2Ma}{Ch_s} \\ -\frac{Ch_s'T_s'}{h_s^2} + \frac{BiCT_s}{h_s^2} & 0 & -\frac{h_s'}{h_s} \end{pmatrix}, \quad \mathbf{E} = \begin{pmatrix} \frac{h_s'}{h_s} & 0 & 0 \\ 0 & 0 & 0 \\ 0 & 0 & 0 \end{pmatrix}$$

and $\mathbf{D} = \mathbf{I}$, as \mathbf{I} is the identity matrix.

Since the conditions (3.6) are homogeneous boundary conditions for \mathbf{v} and \mathbf{w} , only the half interval $x \in [0, 1]$ is considered. Then the boundary conditions (3.6) can be written as:

$$(A.5) \quad \mathbf{v}(0) = \mathbf{0},$$

$$(A.6) \quad \mathbf{w}(1) = \mathbf{0}.$$

The unknown vector \mathbf{v} is sought in the form:

$$(A.7) \quad \mathbf{v}(x) = \mathbf{A}(x)\mathbf{w}(x),$$

where $\mathbf{A}(x) = \{A_{ij}(x)\}$, with $i, j = 1, 2, 3$, is an unknown matrix, whose elements will be found after solving the differential equation:

$$(A.8) \quad \mathbf{A}' = \mathbf{G} - \mathbf{A}\mathbf{E} + (\mathbf{K}-\mathbf{A}\mathbf{D})\mathbf{A}$$

with the homogeneous boundary condition:

$$(A.9) \quad \mathbf{A}(0) = \mathbf{0}.$$

The solution of (A.8), (A.9) represents the direct differential Gauss elimination. The inverse differential Gauss elimination can be similarly constructed from $x = 1$ towards $x = 0$. Both eliminations are matched at some inner point $x_c \in (0, 1)$, which leads to an eigenvalue condition (characteristic equation) containing the elements of the two matrices: the direct elimination matrix (\mathbf{A}) and the inverse elimination matrix. The elements of both matrices are found numerically by the Runge-Kutta method. The eigenvalue is sought iteratively from the obtained characteristic equation using the secant method, which is fast converging.

REFERENCES

- [1] ORON, A., S. H. DAVIS, S. BANKOFF. Long-Scale Evolution of Thin Liquid Films. *Rev. Mod. Phys.*, **69** (1997), 931–980.
- [2] CRASTER, R. V., O. K. MATAR. Dynamics and Stability of Thin Liquid Films. *Rev. Mod. Phys.*, **81** (2009), 1131–1198.
- [3] GROMYKO, G., S. TABAKOVA, L. POPOVA. On the Cooling of a Free Thin Film at the Presence of the van der Waals Forces. *Mathematical Modelling and Analysis*, **9** (2004), No. 4, 299–312.
- [4] TABAKOVA, S., G. GROMYKO. Numerical Modelling of the Free Film Dynamics and Heat Transfer under the van der Waals Forces Action. *Lecture Notes in Comp. Science*, **3401** (2005), 511–518.
- [5] BOWEN, M., B. S. TILLEY. Thermally Induced van der Waals Rupture of Thin Viscous Fluid Sheets. *Phys. Fluids*, **24** (2012), 032106-1–032106-19.
- [6] TABAKOVA, S. Dynamics and Stability of Free Thin Films. *AIP Conference Proceedings*, **1301** (2010), 531–542.
- [7] TABAKOVA, S. Nonlinear Dynamics and Stability of Thin Films with Insoluble Surfactants. *Journal of Theoretical and Applied Mechanics*, **41** (2011), No. 3, 43–58.
- [8] ERNEUX, T., S. H. DAVIS. Nonlinear Rupture of Free Films. *Phys. Fluids*, A **5** (1993), No. 5, 1117–1122.